Bose-Einstein correlations in e^+e^- annihilations in the Υ region

P. Avery, C. Bebek, K. Berkelman, D. G. Cassel, T. Copie, R. DeSalvo, J. W. DeWire, R. Ehrlich, R. S. Galik, M. G. D. Gilchriese, B. Gittelman, S. W. Gray, A. M. Halling, D. L. Hartill, B. K. Heltsley, S. Holzner, M. Ito, J. Kandaswamy, D. L. Kreinick, Y. Kubota, N. B. Mistry, E. Nordberg, M. Ogg, D. Peterson, D. Perticone, M. Pisharody, K. Read, A. Silverman, P. C. Stein, S. Stone, and Xu Kezun
Cornell University, Ithaca, New York 14853

A. J. Sadoff
Ithaca College, Ithaca, New York 14850

T. Bowcock, R. T. Giles, J. Hassard, K. Kinoshita, F. M. Pipkin, and Richard Wilson
Harvard University, Cambridge, Massachusetts 02138

P. Haas, M. Hempstead, T. Jensen, H. Kagan, and R. Kass
Ohio State University, Columbus, Ohio 43210

S. Behrends, T. Gentile, Jan M. Guida, Joan A. Guida, F. Morrow, G. Parkhurst, R. Poling, C. Rosenfeld, E. H. Thorndike, and P. Tipton
University of Rochester, Rochester, New York 14627

D. Besson, J. Green, R. Namjoshi, F. Sannes, P. Skubic,* and R. Stone
Rutgers University, New Brunswick, New Jersey 08854

D. Bortoletto, A. Chen, M. Goldberg, N. Horwitz, A. Jawahery, P. Lipari, P. Lubrano, G. C. Moneti, C. G. Trahern, and H. van Hecke
Syracuse University, Syracuse, New York 13210

S. E. Csorna, L. Garren, M. D. Mestayer, R. S. Panvini, G. B. Word, and Xia Yi
Vanderbilt University, Nashville, Tennessee 37235

M. S. Alam
State University of New York at Albany, Albany, New York 12222

A. Bean and T. Ferguson
Carnegie-Mellon University, Pittsburgh, Pennsylvania 15213
(Received 22 April 1985)

We have used the CLEO detector to study Bose-Einstein (BE) correlations among charged pions produced in the hadronic decays of the $\Upsilon(1S)$ and in continuum e^+e^- annihilations around $\sqrt{s}=10.5$ GeV. We discuss different parametrizations of the effect, and find indications that the production of long-lived particles in these events can account for the observed reduction of the strength of the effect. We determined source dimensions of quark and gluon jets. From the standpoint of BE correlations, we see no difference between the hadronization of quarks and gluons.

I. INTRODUCTION

In the late 1950s, Goldhaber, Goldhaber, Lee, and Pais (GGLP) observed a difference between two-particle distributions of like- and unlike-sign pions produced in the annihilation of protons and antiprotons, and showed that this difference was related to the finite size of the pion source.[1] Since then the study of Bose-Einstein (BE) correlations has been used to probe the spacetime structure of πp, Kp, pp, $p\bar{p}$, $\alpha\alpha$ (Refs. 2–5), e^+e^- (Refs. 6–9), and heavy-ion[10–14] collisions. With this technique, we can measure the size and shape of the volume in spacetime from which particles originate. In the Υ region we have the opportunity to compare BE correlations in the direct decay of the $\Upsilon(1S)$ with those of the continuum nearby, and make inferences about quark and gluon hadronization. In e^+e^- annihilations, pions are produced in the hadronization of quarks and gluons directly, or in the decay of heavier objects produced in the hadronization. From the measured size of the production volume, as well as from the strength of the BE effect, we may learn about the nature of quark and gluon hadronization.

In Sec. II we give an overview of the theory, where we discuss different parametrizations. We discuss different methods for obtaining a reference sample. In Sec. III we describe analysis cuts and the effects of detector resolution, and in Sec. IV the results of the analysis are presented. We present an estimate of the reduction of the observed strength of the BE effect due to the presence of long-lived particles in our sample. Section V contains our conclusions.

II. THEORETICAL OVERVIEW

We picture the production of pions in the hadronization of quarks and gluons as occurring at spacetime points x inside some finite spacetime volume. The distribution of these production points is described by a function $f(x)$, and can be characterized by a radius of a four-dimensional volume. The situation is schematically depicted in Fig. 1. We consider two pions, with the same charge, produced at points x_A and x_B (Ref. 15). They are observed at detectors 1 and 2, with four-momenta p_1 and p_2, respectively. We assume that we can describe the pions by plane-wave functions. Because of the ambiguity in the origin of the pions, the wave function describing the two pions has to be properly symmetrized, and reads

$$\Psi=\frac{1}{\sqrt{2}}(\Psi_{1A}\Psi_{2B}+\Psi_{1B}\Psi_{2A}) , \tag{1}$$

where Ψ_{1A} is the wave function for a pion produced at x_A and traveling to detector 1, and so on. The probability density $I_{\rm BE}\equiv|\Psi|^2$ takes the form

$$I_{\rm BE}=1+\cos[(p_1-p_2)(x_A-x_B)] . \tag{2}$$

$I_{\rm BE}$ is a function of the four-momentum difference, and this distribution is characterized by a parameter (x_A-x_B). For a reference sample consisting of opposite-sign pions, no symmetrization is necessary, and $I_{\rm ref}=1$. The Bose-Einstein ratio $R_{\rm BE}$ is the ratio of the two probabilities

$$R_{\rm BE}=I_{\rm BE}/I_{\rm ref} . \tag{3}$$

In this ratio, most two-particle production features such as phase space will divide out (but not certain final-state-interaction and resonance-decay effects), so that our conclusions are relatively independent of the actual shape of the one- and two-particle distributions. When we generalize from two point sources x_A and x_B to the distribution of pion production points x described by $f(x)$, $R_{\rm BE}$ takes the form

$$R_{\rm BE}(p_1,p_2)=1+|G[f(x)]|^2 , \tag{4}$$

where

$$G[f(x)]=\int f(x)e^{-(p_1-p_2)\cdot x}dx$$

is the Fourier transform of $f(x)$. Thus by studying the correlations between the momenta of pion pairs we can determine the distribution of the points of origin of the pions.

A. The Goldhaber parametrization

Leaving a precise description for $f(x)$ aside for the moment, we write (4) in the form first proposed[1] by GGLP:

$$R_{\rm BE}=1+\exp(-\beta Q^2) , \tag{5}$$

where

$$Q^2=-(p_1-p_2)^2=M^2-4m_\pi{}^2 .$$

M is the invariant mass of the two pions. We can interpret $\sqrt{\beta}$ as the rms radius r of the spacetime volume in which pions are produced. Converting to SI units, $r=0.197\sqrt{\beta}$ fm (with β in GeV^{-2}). Q^2 is obviously a relativistic invariant. If we fix a direction in our two-particle system, we can find one more independent invariant quantity, and we can introduce another independent parameter (γ). Following Kopylov,[16] we introduce q_T, q_L, and q_0, defined in Fig. 2, and rewrite (5) as

$$R_{\rm BE}=1+\exp[-\beta q_T{}^2-\gamma(q_L{}^2-q_0{}^2)] . \tag{6}$$

q_L (q_T) is the component of the three-momentum difference parallel (transverse) to the average momentum $\mathbf{p}_{\rm av}=(\mathbf{p}_1+\mathbf{p}_2)/2$. q_T and $(q_L{}^2-q_0{}^2)$ are relativistically invariant with respect to boosts along $\mathbf{p}_{\rm av}$. Equation (5) and the expanded form (6) will subsequently be referred to as the Goldhaber parametrization.

B. The Kopylov parametrization

Kopylov and Podgoretsky[16,17] and Cocconi[15] introduced a parametrization that has found widespread use in the interpretation of experimental results.[2–5,11,13,14] In this paper, it will be referred to generically as the Kopylov parametrization. Their model for the source of the interfering pions is a spherical surface of radius R populated with pion radiators of lifetime τ. Using the general equation (4), this leads to

$$R_{\rm BE}=1+I^2(qR)\frac{1}{1+(q_0\tau)^2} , \tag{7}$$

where $I(y)=2J_1(y)/y$, J_1 being the first-order Bessel function. $q=|\mathbf{p}_1-\mathbf{p}_2|$ and $q_0=E_1-E_2$, as before. The aim of this parametrization is to extract from the data not

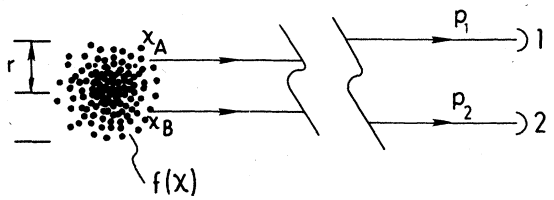

FIG. 1. Schematic representation of the BE effect.

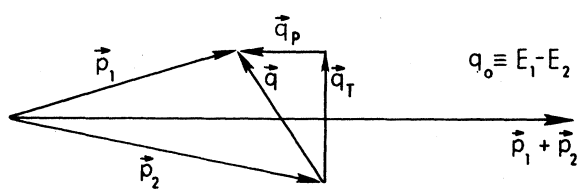

FIG. 2. Definition of the Kopylov variables.

only the radius R of the source distribution, but also the scatter in time τ of the production times. In most applications, q_T is used in Eq. (7) instead of q. The advantage of this is that q_0 and q_T are independent variables, whereas q_0 and q are correlated: particles are restricted to roughly half of the q_0-q plane.

C. Comparison of the Goldhaber and Kopylov forms

In order to facilitate comparison of Eq. (7) with Eq. (6), we make some substitutions. The function I^2 in (7) is virtually indistinguishable from a Gaussian.[1] The term involving q_0 is likewise a rapidly falling function, and can also be approximated by a Gaussian. Furthermore, we split the three-momentum difference q into q_T and q_L. Equation (7) can now be written

$$R_{\mathrm{BE}}=1+\exp[-\beta(q_T{}^2+q_L{}^2)-\delta q_0{}^2] . \tag{8}$$

This is also obtained from (4) assuming $f(x)$ to be a Gaussian in four dimensions. δ is approximately $0.7\tau^2$. Equation (8) should be compared with Eq. (6). The essential difference between the two formulations is in the sign of the q_0 term. This means that we cannot write the Kopylov parametrization in a relativistically invariant form, as we did with the Goldhaber parametrization. On the experimental side, the difference between (8) and (6) should be readily visible, because q_0 and q_L are strongly correlated. To show this, we first define $p=p_1+p_2$, $q=p_1-p_2$, the sum and difference of the four-momenta. For equal (pion) masses m, $p\cdot q=0$; therefore,

$$p_0q_0=\mathbf{p}\cdot\mathbf{q}=|\mathbf{p}|q_L .$$

Then

$$q_0=q_L\frac{|\mathbf{p}|}{p_0}=q_L\frac{|\mathbf{p}|}{(M^2+|\mathbf{p}|^2)^{1/2}}=q_L\frac{|\mathbf{p}|}{(4m^2+4p^{*2}+|\mathbf{p}|^2)^{1/2}} . \tag{9}$$

Here, M is the invariant mass of the two pions, and p^* is the pion momentum in the dipion center-of-mass frame. m^2 is small compared to $|\mathbf{p}|^2$ for our cuts, and we drop the term. We are left with

$$q_0\cong q_L\frac{1}{\left[1+\dfrac{4p^{*2}}{|\mathbf{p}|^2}\right]^{1/2}} . \tag{10}$$

In our case, p^* is small compared to $|\mathbf{p}|$, and therefore

$$q_0\cong q_L . \tag{11}$$

This leads to an approximate cancellation of the last terms in the exponent of (6), making R_{BE} almost independent of q_0 and q_L. In Fig. 3 we show the normalized ratio of like- and unlike-sign pairs as a function of q_0 for (a) all values of q_T and for (b) q_T restricted to the range 0—0.2 GeV. These distributions are indeed almost flat. Other experiments[11,13,14] have similarly reported that R_{BE} depends only weakly on q_0. In contrast, according to Eq. (8), R_{BE} should show a Gaussian drop as a function of q_0. Both the Goldhaber and the Kopylov form predict the same Gaussian behavior of R_{BE} as a function of q_T. As a result, we have to conclude on both theoretical and experimental grounds that the Kopylov parametrization does not provide a proper framework for the interpretation of our data, and in the subsequent analysis we have used the modified Goldhaber form of Eq. (6).

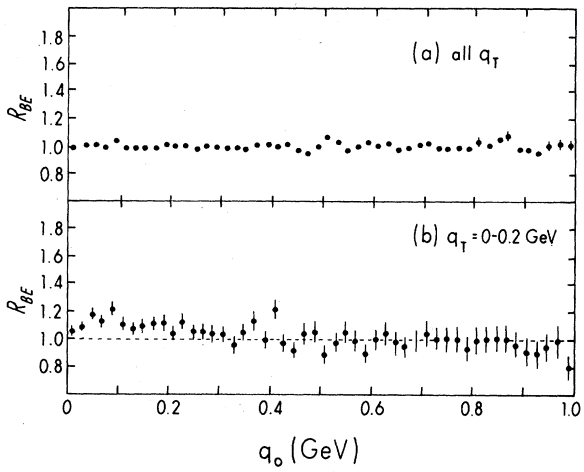

FIG. 3. R_{BE} versus q_0 for (a) all q_T, and (b) q_T=0—0.2 GeV.

D. The strength of the BE effect

Equation (6) tells us that the value of R_{BE} should be 2 in the limit q_0, q_T, and $q_L\to 0$. Experimentally, this is not the case. Therefore, (6) is modified:

$$R_{\mathrm{BE}}=1+\alpha\exp[-\beta q_T{}^2-\gamma(q_L{}^2-q_0{}^2)] . \tag{12}$$

The parameter α in Eq. (12) can be interpreted as indicating the strength of the BE effect. Different effects which can cause α to be less than unity are described later.

E. The reference sample

The choice of a reference sample is a central problem in the experimental study of Bose-Einstein correlations. Ideally, this sample should be identical to the same-sign pion-pair sample in all respects except for the BE correlations. Many different techniques can be used to obtain such a sample, and we have examined a number of these. Several methods will be described below.

One of the simplest ways to obtain a reference sample of pion pairs that will not exhibit BE correlations is to use the unlike-sign pion pairs in the events. The production dynamics of negative and positive pions in e^+e^- annihilations are identical in most respects, so the properties of randomly chosen unlike-sign pairs and like-sign pairs should be the same, except for BE correlations and correlations arising from resonance decays (primarily K^0 and ρ^0) and photon conversions. We have to take care that the latter correlations do not affect our results. Fortunately, the most important contaminations, due to K^0 and ρ^0, affect well-specified regions in our distributions, and can therefore be easily dealt with. Converted photons contam-

inate the q_T distributions below $q_T=0.12$ GeV, and we exclude this region from our fits. Similarly, ρ^0 decays will not affect our measurements if we exclude the q_T region above 0.62 GeV. K^0 decays produce pion pairs with $Q=0.41$ GeV; hence we exclude pairs between $Q=0.40$ and 0.42 GeV. We have also studied the effect of other resonances, namely, η and ω decays that cause a calculable enhancement of the opposite charge distribution in the region $0<q_T<0.60$ GeV. The effect of these states, that has not been examined in previous similar experiments, will be discussed in Sec. IV A together with that of charge conservation.

Monte Carlo studies show that there is no difference in detector acceptance for like- and unlike-sign pairs in the q_T,q_0 region of interest.

Another method used to obtain a non-BE correlated reference sample is to mix tracks from different events. For this method to work, the events must be isotropic so that there is no preferred direction, or the jet axes must be oriented in the same direction. We only have a limited ability to determine jet axes in the Υ region, where events are neither completely isotropic nor extremely jetlike. The result of this limitation is that the reference events, being composed of tracks from imperfectly aligned events, will end up looking more spherical than the (unmixed) "signal events."

A related method that can be used in events with a clear event axis is to shuffle the momentum components transverse to the axis.[3] As with the event-mixing method, the uncertainty in the determination of an axis in our events leads to a distortion of $R_{\rm BE}$ and additional uncertainty about the proper parametrization. This is detailed in Appendix B.

Using Monte Carlo simulation of the hadronization process to produce a reference sample leads to similar distortions of $R_{\rm BE}$. This is not entirely surprising, since the models typically are not tuned to two-particle distributions.

The examination of various methods and the arguments given in the preceding paragraphs have led us to choose the unlike-sign pion pairs from the data as our reference sample. We are confident that unlike-sign pion pairs form a suitable reference sample if we exclude contaminated regions from our calculations, as detailed above.

III. DATA SAMPLE AND TRACK SELECTION

We have used data obtained with the CLEO detector, operating at the Cornell Electron Storage Ring. The detector consists of a 2-m-diameter cylindrical drift chamber inside a 1-T superconducting solenoid. Outside the magnet are particle identification detectors. The CLEO detector,[18] as well as the hadronic event selection criteria[19] have been described in detail elsewhere.

The data samples used in this analysis are summarized in Table I. The last sample was taken in our recent scan above the $\Upsilon(4S)$.[20] For our purposes, we can regard these data as two-jet events with a small admixture of B (B^*) decays. These decays contribute only about 10% to the cross section.[20]

For these three samples, the number of charged tracks that are used in this analysis averages about eight per event. For this analysis, we required charged multiplicity to be at least 5. Individual track momenta were required to be above 0.2 GeV/c. This cut eliminates particles that spiral around in the tracking chamber and make many parallel tracks. The (vector) sum of the two-track momenta that make up a pair was required to be above 0.4 GeV/c. This eliminates possible distortions of $R_{\rm BE}$ due to final-state interactions.[21] All tracks that were identified as other than pions by the dE/dx and time-of-flight systems were rejected.

TABLE I. Data samples.

Region	$\langle E_{\rm c.m.}\rangle$ (GeV)	$\int L$ (nb^{-1})	Hadronic events
$\Upsilon(1S)$	9.5	3505	78363
Continuum $<\Upsilon(4S)$	10.5	18161	58632
Continuum $>\Upsilon(4S)$	10.8	60584	192023

A. Detector resolution

The radii of the pion source regions are determined from the widths of the Gaussian enhancements in the plots of the ratio of like- and unlike-sign pion pairs. The narrower the Gaussian, the larger the radius. The maximum radius that can possibly be determined from our data is given by the two-track resolution, which can be estimated from Monte Carlo simulations of the detector. In Fig. 4 we have plotted the difference between q_T calculated from the momenta given by the event generator, and q_T as calculated from the reconstructed tracks. The distribution has a full width at half maximum (FWHM) of $\delta q_T=0.023$ GeV/c. An estimate of the maximum radius is thus

$$r_{\rm max}=\hbar c\left[\frac{\ln 2}{\delta {q_T}^2}\right]^{1/2}=7\ \text{fm}\ . \tag{13}$$

This is comfortably outside the 1-fm range of values that we expect to encounter.

The finite momentum resolution will broaden any Gaussian enhancement, leading to an underestimate of the measured radius. However, for radii of the order of 1.0 fm, the systematic error introduced by this is less than 1%.

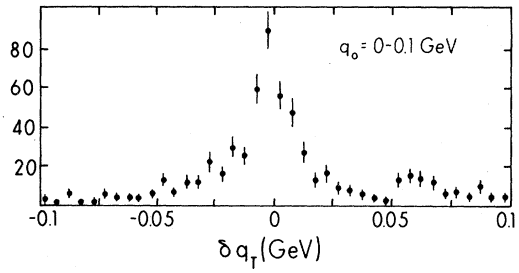

FIG. 4. Detector resolution in q_T.

IV. RESULTS OF THE ANALYSIS

Referring back to Eq. (12), which is repeated here,

$$R_{\rm BE}=1+\alpha\exp[-\beta q_T{}^2-\gamma(q_L{}^2-q_0{}^2)]\ , \tag{12}$$

we see that the Bose-Einstein ratio $R_{\rm BE}$ is a function of q_T and $(q_L{}^2-q_0{}^2)$, and that there are three parameters that describe the correlations in this framework. In our data the close correlation between q_L and q_0 make it impossible to determine γ from our data.

The parameter α indicates the strength of the effect, and ranges between 0 and 1. The parameter β, associated with the square of the transverse-momentum difference q_T, measures the radius of the pion source transverse to the "line of sight." Notice that the radius r that we derive from measurements of β is a radius in three-space, whereas in the original Goldhaber formulation, it is a four-dimensional quantity. Equation (12) tells us that if we let q_0 go to 0 (and implicitly, $q_L\to 0$), then $R_{\rm BE}$ is a function of α and β only. The procedure we followed to extract these two parameters from the data is to plot $R_{\rm BE}$ as a function of q_T in successive 0.1-GeV-wide intervals of q_0. This ratio is normalized such that the numbers of like- and unlike-sign pairs are equal above $q_T=0.3$ GeV. This value is chosen because the BE effect is concentrated below $q_T=0.3$ GeV. The function we use to fit the data to is

$$R_{\rm BE}=A\,[1+\alpha\exp(-\beta q_T{}^2)]\ . \tag{14}$$

The factor A is inserted for the purpose of overall normalization of the fit. Since the ratio of the distributions is already normalized, the value of A in our fits is within a few percent of unity.

A. The continuum data near $\sqrt{s}=10.5$ GeV

Figure 5 shows the distribution of q_T for like-sign and unlike-sign pairs. Nothing dramatic is apparent. However, when we take the ratio of the like- and unlike-sign distributions, the BE effect stands out clearly. Figures 6(a)—6(c) show the normalized ratio for three slices in q_0. The fits are done according to Eq. (14). It is clear that the statistics deteriorate with increasing q_0. The data have been fit in the interval 0.12—0.62 GeV. As discussed above, the region below 0.12 GeV is excluded because of contamination of the unlike-sign sample with converted photons, and the region above 0.62 GeV is excluded because of possible correlations among decay products of the ρ meson. Table II(a) contains the parameters of the fits. All errors given are statistical only. We estimate the systematic error introduced by analysis cuts to be 10% for α and 5% for r.

As indicated in Sec. II E, we have also examined the effect of the contribution of η and ω decays to the reference sample. $e^+e^-\to q\bar{q}$ events were generated with the Lund Monte Carlo, with parameters tuned to our experimental results; on the average it generated 0.70 η/event and 0.41 ω/event. The q_T distributions for the unlike pion pairs from their decays were then subtracted from the unlike-pion-pairs data samples, and Table II(b) displays the fitted parameters when using this subtracted reference distribution. One notices that, when extrapolated to $q_0=0$, the value of α increases by about 30% while the value of r is about 0.72 of the unsubtracted one; the same is approximately true for the other two samples discussed in Sec. IV B. Our knowledge of the number of η's and ω's per event is, however, very uncertain. For this reason, and also for the purpose of comparison with previous results, we will present in the following discussions only the results obtained without subtracting the estimated effect of η and ω decays.

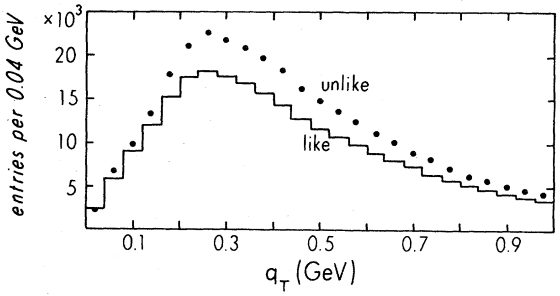

FIG. 5. Yield of like and unlike pairs vs q_T.

In order to estimate possible differences in the like-pion

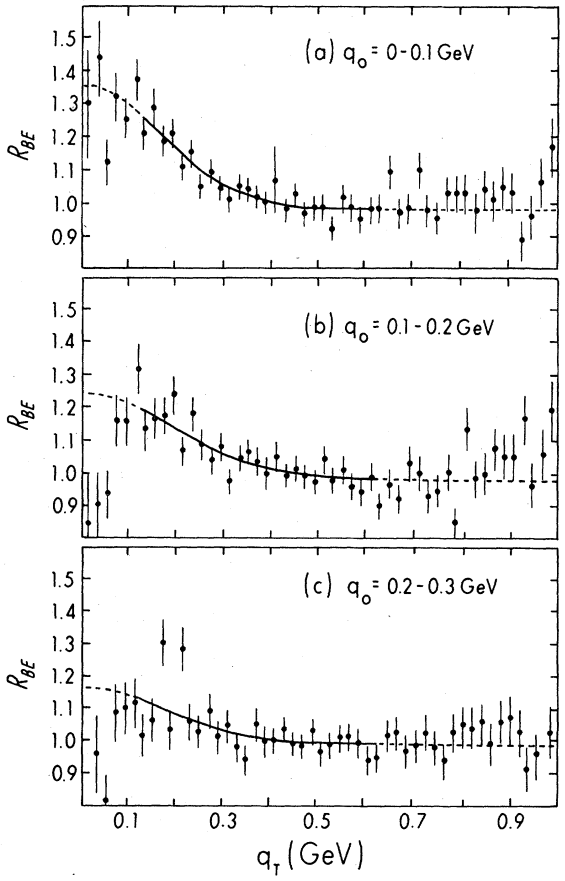

FIG. 6. $R_{\rm BE}$ versus q_T for (a) $q_0=0$—0.1, (b) $q_0=0.1$—0.2, and (c) $q_0=0.2$—0.3 GeV. The curves are fitted in the interval 0.12—0.62 GeV according to Eq. (14).

TABLE II. (a) Fit parameters. (b) Fit parameters with subtraction.

		(a)		
q_0 (GeV)	α	β (GeV^{-2})	χ^2/DF	r (fm)
0.0–0.1	0.38±0.06	18.3±4.6	13/(26−3)	0.84±0.11
0.1–0.2	0.26±0.06	13.9±5.4	19/(26−3)	0.74±0.14
0.2–0.3	0.17±0.06	15.1±9.6	36/(26−3)	0.77±0.24
		(b)		
q_0 (GeV)	α	β (GeV^{-2})	χ^2/DF	r (fm)
0.0–0.1	0.51±0.05	9.74±2.2	16/(26−3)	0.62±0.07
0.1–0.2	0.45±0.05	7.40±2.2	22/(26−3)	0.54±0.08
0.2–0.3	0.35±0.05	9.40±3.5	38/(26−3)	0.60±0.11

and unlike-pion distributions due to charge conservation effects, we have divided this sample (as well as the ones discussed below) into events with charged track multiplicity less or equal to 7, and events with charged multiplicity greater than 7. We expect any charge-conservation effects to show more strongly in the lower-multiplicity subsample. The fitted values of α and r for the two subsamples differ by considerably less than the statistical errors and we conclude that charge-conservation effects are negligible at the current level of accuracy.

Since $R_{\rm BE}$ is a slowly varying function of q_0, we extrapolate linearly the values of r and α obtained in the three plots of Fig. 6 to $q_0=0$. The results are

$$r=0.86\pm0.15 \text{ fm},$$

$$\alpha=0.43\pm0.07 .$$

The low value of α indicates that the BE effect is not complete, and that a substantial fraction of the pions do not participate in the BE interference.

B. Results from the $\Upsilon(1S)$ and the continuum above the $\Upsilon(4S)$

The same procedures have been applied to the data samples of the $\Upsilon(1S)$, and the continuum above the $\Upsilon(4S)$. In the case of the $\Upsilon(1S)$, a subtraction was performed to remove the continuum background and the fraction of the $\Upsilon(1S)$ that decays into $q\bar{q}$. Table III gives the values of α and the radius r for the $\Upsilon(1S)$, the continuum (for comparison), and the continuum above the $\Upsilon(4S)$. We see that the radius r from the $\Upsilon(1S)$ data looks slightly larger than that for the continuum data, although these radii are certainly all within errors of each other. The parameters of the continuum below and above the $\Upsilon(4S)$ are the same within errors, as we expect. The values of α are far below the theoretical maximum of 1.

TABLE III. α and r for different data samples.

	α	r (fm)
$\Upsilon(1S)$	0.50±0.09	0.99±0.14
Continuum $<\Upsilon(4S)$	0.43±0.07	0.86±0.15
Continuum $>\Upsilon(4S)$	0.41±0.04	0.86±0.08

C. Correction to α for presence of long-lived resonances

We have investigated the extent to which deviations of α from unity may be due to the fact that some pions are the decay products of particles which have traveled far from the primary hadronization region before decaying. Interference involving these pions would lead to enhancements of $R_{\rm BE}$ that are two narrow for observation, producing an effective decrease in α. In Appendix A we present the details of these studies. The main results are that the reduction in strength of the BE effect is severe. On the $\Upsilon(1S)$ this is due mostly to the presence of η's and ω's. On the continuum, there is additional reduction due to charmed particles. In Fig. 7 we have plotted the ratio k of the true α and the observed α. Thus k can be interpreted as an upper limit on the observed value of α. Values of k are around 0.4 and 0.3 for the $\Upsilon(1S)$ and the continuum, respectively. We can use these values of k to correct the data points in Fig. 6(a) upwards. The result is Fig. 8. The value of α in the fit is now 1.45±0.25. Although this is more than the allowed maximum of 1, a good fit can still be obtained with α fixed at 1. Table IV shows the results of the fits for the continuum and $\Upsilon(1S)$ data. Our estimate of the effect is of course model dependent to an extent difficult to estimate; however, these cases show that this effect alone seems to be sufficient to account for the observed values of α in our data. They suggest that the BE effect is fully effective in the primary hadronization of quarks and gluons. This also means that there is little room left for other effects that can lower the value of α.[22]

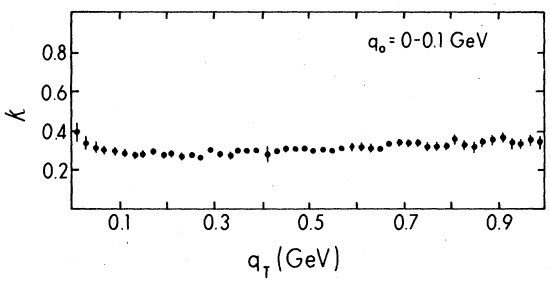

FIG. 7. The ratio k of observed α to real α for the continuum.

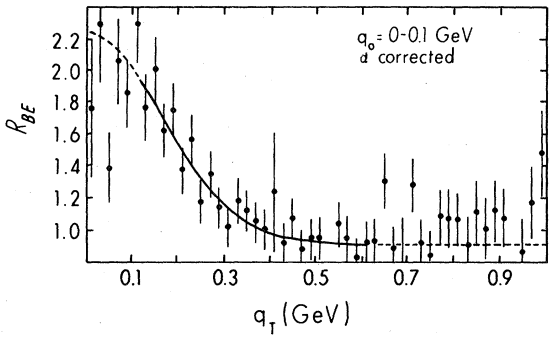

FIG. 8. R_{BE} for continuum, with α corrected.

D. The shape of quark and gluon jets

In the next phase of the analysis, we attempt to isolate single-gluon and quark jets and measure their dimensions transverse and parallel to the jet axis. We are sensitive to spatial dimensions parallel to the momentum difference vector. Therefore if we restrict q_T to be parallel (transverse) to the jet axis, we measure the size of the pion-source region parallel (transverse) to this axis. In our analysis, "parallel" (transverse) means that q_T makes an angle of less (more) than 45° with the jet axis. The jets were defined using the triplicity variable,[23] which divides an event into three jets. We needed the triplicity for the $\Upsilon(1S)$ to identify the three-gluon jets. Since we wanted to make a direct comparison with the continuum, we used the same shape analysis there. The continuum event axis is then given by the major triplicity axis.

For this comparison, we only look at the highest-energy jet, since in the three-gluon decay of the $\Upsilon(1S)$ the jets formed by the two least energetic gluons are expected to overlap to a great extent. Table V shows the transverse dimensions for quark and gluon jets. The transverse sizes are the same within errors. We were not able to determine the longitudinal dimensions due to the paucity of pions moving transverse to the jet axis with appreciable momentum.

Finally, we can compare the "weak halves" of the events, the part of the events left over after the most energetic jet has been taken out. On the $\Upsilon(1S)$, this "weak half" is expected to be the effect of two diverging gluons, and therefore the combined pion-source region is expected to be wider (in the event plane defined by the three jets) than on the continuum, where it consists of just one jet. For this comparison, $\mathbf{q}_T$ was therefore also restricted to be within 45° of the event plane. Table VI shows the transverse dimensions of the weak halves: The weak half on the $\Upsilon(1S)$ indeed seems to be wider than on the continuum. Taken together with the results in Table V, this supports our picture of the $\Upsilon(1S)$ as a three-jet structure.

It should be noted that the values of r in Tables V and VI represent an average of radii as measured along the direction of q_T, with q_T restricted to some angular range. If the pion-source distribution is ellipsoidal, with the major axis along (perpendicular to) the jet axis, the size of the measured radius will be larger (smaller) than the minor axis of the pion-source distribution because of this averaging.

TABLE IV. Corrected values of α.

	α	χ^2/DF
Continuum	1.45±0.25	13/(26−3)
Continuum	1 (fixed)	18/(26−2)
$\Upsilon(1S)$	1.20±0.23	21/(26−3)
$\Upsilon(1S)$	1 (fixed)	22/(26−2)

TABLE V. Transverse dimensions of q,g jets.

		α	r (fm)
q	(continuum)	0.42±0.10	0.73±0.12
g	($\Upsilon(1S)$)	0.46±0.11	0.80±0.20

V. CONCLUSIONS

(1) We can compare our measurements with those made in e^+e^- experiments at different energies. Table VII lists values of α and r that have been obtained. The observed radii are all around 0.8 fm, and seem to be independent of c.m. energy over a range of almost an order of magnitude. Unfortunately, there are no theoretical predictions for r (in e^+e^- experiments), nor for its dependence on $E_{\text{c.m.}}$.

(2) The Kopylov parametrization does not adequately describe our data.

(3) The average radii of the pion-producing volumes are 0.99±0.14 and 0.86±0.09 fm for the $\Upsilon(1S)$ and the continuum, respectively. These values should be reduced by a factor of around 0.7 when the effect of η and ω decay in the reference sample is taken into account.

(4) The presence of long-lived resonances in the sample can account for the observed values of the parameter α, leaving little room for other effects that would lower the value of α. This suggests that the Bose-Einstein interference is fully effective for the pions produced in quark and gluon hadronization.

(5) As for individual jets, the transverse dimensions of quark and gluon jets are the same within errors, about 0.8 fm, slightly smaller than the average radii of the whole events. Taken together with the observation that the weak half of the $\Upsilon(1S)$ has a wider source distribution than for the continuum, this supports our picture of the $\Upsilon(1S)$ and the continuum as three- and two-jet structures, respectively.

Thus Bose-Einstein correlations do not reveal a dramatic difference between quark and gluon hadronization.

TABLE VI. Transverse dimension of "weak" event half.

	α	r (fm)
Continuum	0.43±0.09	0.74±0.15
$\Upsilon(1S)$	0.69±0.13	1.11±0.17

TABLE VII. α and r for different energies.

$E_{c.m.}$ (GeV)	α	r (fm)
3.1[a]	0.71±0.03	0.85±0.02
4–7[a]	0.52±0.06	0.77±0.08
29[b]	0.51±0.06	0.65±0.18
34[c]	0.30±0.08	0.94±0.17
34[d]	0.72±0.08	0.79±0.06

[a]Goldhaber (Ref. 6).
[b]Aihara *et al.* (Ref. 9).
[c]Koch (Ref. 7).
[d]These are the same data as in the preceding table entry, but a Monte Carlo reference sample was used.

ACKNOWLEDGMENTS

It is a pleasure to thank the Cornell Electron Storage Ring operating staff for their dedicated efforts. This work was supported by the National Science Foundation and the Department of Energy. One of us (M.G.D.G) would like to thank the Alfred P. Sloan Foundation for support. One of us (H.K.) acknowledges the Department of Energy's OJI program for support.

APPENDIX A: REDUCTION OF α BY LONG-LIVED PARTICLE DECAY

In this appendix we estimate the reduction of α due to the fact that some pions are the decay products of particles which have traveled far from the primary hadronization region before decaying. The pions in our events can be divided into two classes: (1) those that are primary pions or are the decay products of short-lived resonances such as the ρ^0, and (2) those pions that are produced in the decay of long-lived resonances such as charmed particles, η and ω. We can expect interference among the pions of class (1), and among the pions produced in the decay of the same long-lived resonance, but we do not expect interference[24] between pions of mixed origin: one primary and another from a long-lived parent particle, or both from different long-lived particles. We have used Monte Carlo studies to investigate this effect and estimate an upper limit on α.

We give the subscript i to numbers referring to pion pairs that can interfere, and the subscript ni to quantities referring to pion pairs of mixed origin which cannot interfere. Superscripts l,u are for like- and unlike-sign pairs. The BE effect can be measured by the ratio of like/unlike-sign pairs n_i^l/n_i^u at very low q_T, where the effect is maximal, normalized to the number of like/unlike-sign pairs N_i^l/N_i^u at higher q_T, where no effect is expected:

$$\frac{n_i^l}{n_i^u}\Big/\left[\frac{N_i^l}{N_i^u}\right]=1+\alpha\ . \tag{A1}$$

Of course, for the pairs of mixed origin, we expect no effect:

$$\frac{n_{ni}^l}{n_{ni}^u}\Big/\left[\frac{N_{ni}^l}{n_{ni}^u}\right]=1\ ; \tag{A2}$$

TABLE VIII. Properties of parent particles.

	Continuum		$\Upsilon(1S)$	
Particle	Fract.	$\langle p\rangle/\Gamma M$ (fm)	Fract.	$\langle p\rangle/\Gamma M$ (fm)
D,F[a]	15	∞	0	
η	3.4	450	3.3	340
η'	1.5	900	1.4	700
ω	8	22	7	21
ϕ	0.1	48	0.2	46

[a]These include D^0, $\overline{D}^0$, D^+, D^-, F^+, F^-, D^{*+}, D^{*0}, and D^{*-}.

and for the whole data set, we expect a diluted BE effect:

$$\frac{n_i^l+n_{ni}^l}{n_i^u+n_{ni}^u}\Big/\left[\frac{N_i^l+N_{ni}^l}{N_i^u+N_{ni}^u}\right]=1+\alpha'\ , \tag{A3}$$

where α' should be smaller than α. If we write $\alpha'=k\alpha$, k can be expressed in terms of the various n and N. The value of k, which measures the dilution of a potential BE effect due to the admixture of noninterfering particles, can now be estimated from a Monte Carlo simulation, even when the model does not provide for BE interference. For a Monte Carlo model which is known not to contain the BE effect k takes a simple form:

$$k=\frac{n_i^l}{n_i^l+n_{ni}^l}\ . \tag{A4}$$

We have determined k from the Lund Monte Carlo model,[25] which has been tuned to reproduce CLEO data. The criterion that determines whether a particle is considered long-lived is whether the particle can travel far ($\gg 1$ fm) from the primary interaction region. This is determined by the width Γ and mass M of the resonance and its momentum p (Ref. 26):

$$\frac{p}{\Gamma M}\gg 1\text{ fm}\ . \tag{A5}$$

Table VIII contains a list of some particles, with the fraction of times (in %) that these particles play a role as a parent in pair that passes all our cuts, and the average distance traveled before decaying. These numbers are obtained from simulations of event generation and the full detector. On the continuum, production of charmed mesons is possible. These do not play an appreciable role on the $\Upsilon(1S)$. Therefore the dilution of the BE effect on the continuum is more severe than on the $\Upsilon(1S)$. This is reflected in the values of k; for the $\Upsilon(1S)$, k is around 0.4, whereas for the continuum, its value is around 0.3. In Fig. 7 the dilution factor k is plotted as a function of q_T for values of q_0 between 0 and 0.1 GeV for the $\Upsilon(1S)$.

APPENDIX B: MIXING METHODS FOR THE REFERENCE SAMPLE

In this appendix we will describe our findings concerning the construction of a reference sample by mixing momentum components transverse to the event axis. As mentioned in the main text, we have a limited ability to determine this axis. Consequently, the one- and two-

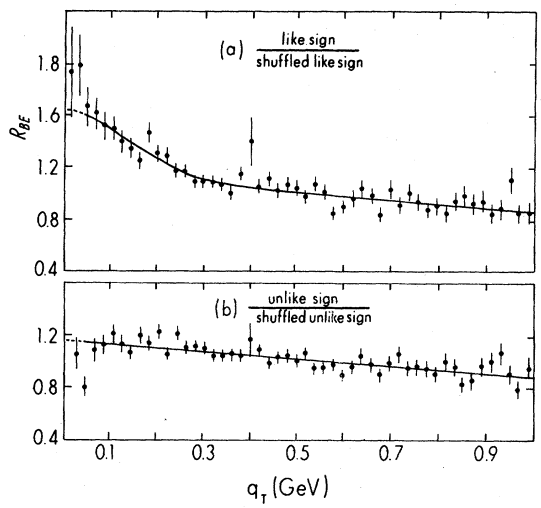

FIG. 9. (a) R_{BE} using a reference sample of shuffled like-sign pairs; the fitted curve is according to Eq. (20), and (b) the ratio of unlike-sign pairs to shuffled unlike-sign pairs.

particle distributions of the reference sample will be affected. This becomes apparent in our analysis in that the ratio of signal to reference distributions does not approach a constant for large q_T, as it should. This is illustrated by Fig. 9(a), which shows the ratio of like-sign pairs to like-sign pairs after the transverse momenta in the event have been shuffled. This should be compared with Fig. 6(a), where the reference sample was made up of unlike-sign pairs. The fits to the data are with the function[27]

TABLE IX. Fit parameters for Figs. 9(a) and 6(a).

	α	r	m
Fig. 9(a)	0.41±0.08	0.81±0.13	−0.24±0.05
Fig. 6(a)	0.38±0.06	0.84±0.11	fixed to 0

$$A(1+mq_T)[1+\alpha\exp(-\beta q_T{}^2)] \ . \tag{B1}$$

Table IX lists the parameters of the fits for Figs. 9(a) and 6(a). Notice that α and r do not differ much between these two fits. This may lend support to the hypothesis that the only apparent difference between the two methods is a linear dependence on q_T for high q_T. We can also take the results of Table IX to obtain an estimate of the systematic errors in α and β due to our choice of the reference sample. They are 7% and 4% for α and r, respectively. For good measure, the ratio of the distribution of unlike-sign pairs to the distribution of the unlike-sign pairs, after their transverse momenta have been shuffled, is shown in Fig. 9(b). The slope of the (straight-line) fit is -0.23 ± 0.03, very close to the slope in Fig. 9(a), as we expect. Because of the uncertainty[27] in the parametrization of the BE effect when we can no longer assume that R_{BE} approaches a constant for large q_T, we have not used the transverse-momentum mixing scheme in further analysis.

Although the arguments given in this appendix were specifically for a transverse-momentum mixing scheme, they apply equally to methods in which tracks are mixed between different events.

*Present address: University of Oklahoma, Norman, OK 73019.

[1]G. Goldhaber, S. Goldhaber, W. Lee, and A. Pais, Phys. Rev. Lett. **3**, 181 (1959); Phys. Rev. **120**, 300 (1960). For a recent review and further references, see also G. Goldhaber, Lawrence Berkeley Laboratory Report No. LBL-19417, 1985 (unpublished).
[2]T. Åkesson *et al.*, Phys. Lett. **129B**, 269 (1983).
[3]M. Deutchmann *et al.*, Nucl. Phys. **B204**, 333 (1982).
[4]C. Ezell *et al.*, Phys. Rev. Lett. **38**, 873 (1977).
[5]S. Barshay, Phys. Lett. **130B**, 220 (1983).
[6]G. Goldhaber, in *Proceedings of the International Conference on High Energy Physics, Lisbon, 1981,* edited by J. Dias de Deus and J. Soffer (European Physical Society, Erice, 1982).
[7]W. Koch, in *Multiparticle Dynamics, 1982,* proceedings of the XIIIth International Symposium, Volendam, The Netherlands, edited by E. W. Kittel, W. Metzger, and A. Stergiou (World Scientific, Singapore, 1983).
[8]R. R. Saurwein, Bull. Am. Phys. Soc. **29**, 740 (1984).
[9]H. Aihara *et al.*, Phys. Rev. D **31**, 996 (1985).
[10]F. B. Yano and S. E. Koonin, Phys. Lett. **78B**, 556 (1978).
[11]S. Y. Fung *et al.*, Phys. Rev. Lett. **41**, 1592 (1978).
[12]W. A. Zajc *et al.*, Phys Rev. C **29**, 2173 (1984).
[13]J. J. Lu *et al.*, Phys. Rev. Lett. **46**, 898 (1981).
[14]D. Beavis *et al.*, Phys. Rev. C **27**, 910 (1983).
[15]G. Cocconi, Phys. Lett. **49B**, 459 (1974).
[16]G. I. Kopylov, Phys. Lett. **50B**, 472 (1974).
[17]G. I. Kopylov and M. I. Podgoretsky, Yad. Fiz. **18**, 656 (1973) [Sov. J. Nucl. Phys. **18**, 336 (1974)].
[18]D. Andrews *et al.*, Nucl. Instrum. Methods **211**, 47 (1983).
[19]S. Behrends *et al.*, Phys. Rev. D **31**, 2161 (1985).
[20]D. Besson *et al.*, Phys. Rev. Lett. **54**, 381 (1985).
[21]M. Gyulassi, S. K. Kauffmann, and L. W. Wilson, Phys. Rev. **20C**, 2267 (1979).
[22]G. N. Fowler and R. M. Weiner, Phys. Lett. **70B**, 201 (1977).
[23]S. Brandt and H. D. Dahmen, Z. Phys. C **1**, 61 (1979).
[24]Strictly speaking, we cannot say that these pions do not interfere. However, the enhancement in plots of q_T due to interference of pions from a resonance that has traveled n fm before decaying has a typical width of $0.16/n$ GeV, which is too narrow for our observation for $n \gg 1$ fm [Eqs. (26) and (28)].
[25]T. Sjöstrand, Comput. Phys. Commun. **27**, 243 (1982).
[26]P. Grassberger, Nucl. Phys. **B120**, 231 (1977).
[27]The assertion that the asymptotic behavior in Fig. 9(a) is a simple linear function of q_T is based solely on the fact that it seems a reasonable thing to do from looking at the figure. There is no theoretical argument. This gives rise to the term $(1+mq_T)$ in (20). Several authors display their data as a function of $q_T{}^2$ rather than q_T. For them, the natural step to take, upon observing that their ratios do not approach a constant for large q_T, is to introduce a factor $(1+mq_T{}^2)$ in their fits (see Refs. 7, 3, 6, and 26). Choosing linearity in q_T or $q_T{}^2$ can affect the values of α and β. For example, allowing for a quadratic term in the fit of Fig. 9(a) can lead to changes in α and β of up to 20%.